Extraction of Airways from CT (EXACT'09)

Pechin Lo[1], Bram van Ginneken[2],
Joseph M. Reinhardt[3], and Marleen de Bruijne[1,4]

[1] Image Group, Department of Computer Science, University of Copenhagen, Denmark, pechin@diku.dk,
[2] Image Sciences Institute, University Medical Center Utrecht, The Netherlands,
[3] Department of Biomedical Engineering, Iowa Institute for Biomedical Imaging, The University of Iowa, USA,
[4] Biomedical Imaging Group Rotterdam, Departments of Radiology & Medical Informatics, Erasmus MC, Rotterdam, The Netherlands

Abstract. This paper describes a framework for evaluating airway extraction algorithms in a standardized manner and establishing reference segmentations that can be used for future algorithm development. Because of the sheer difficulty of constructing a complete reference standard manually, we propose to construct a reference using results from the algorithms being compared, by splitting each airway tree segmentation result into individual branch segments that are subsequently visually inspected by trained observers. Using the so constructed reference, a total of seven performance measures covering different aspects of segmentation quality are computed. We evaluated 15 airway tree extraction algorithms from different research groups on a diverse set of 20 chest CT scans from subjects ranging from healthy volunteers to patients with severe lung disease, who were scanned at different sites, with several different CT scanner models, and using a variety of scanning protocols and reconstruction parameters.

1 Introduction

Analysis of the airways in volumetric computed tomography (CT) scans plays an important role in the diagnosis and monitoring of lung diseases. While airway segmentation is a key component for such analysis, the accuracy and reliability of existing algorithms for segmenting the airway are still unknown because of the lack of a common test database, a reference, and standardized means for comparison.

The aim of this paper is to develop a framework for evaluating airway extraction algorithms in a standardized manner and to establish a database with reference segmentations that can be used for future algorithm development. Because of the sheer difficulty of establishing a complete reference standard manually, we propose to instead construct a reference using results from the algorithms to compare. Airway tree segmentations were first subdivided into their individual branches, which can be easily visualized and were subsequently evaluated by

trained observers. This way, manual annotation is avoided and the trained observer is given the easier task of deciding whether a segmented branch is correct or wrong, thus separating wrongly labeled regions from correctly labeled regions. We focus the evaluation on extracting the most complete airway trees, progressing into higher generation airways and extracting as many branches as possible. The exact airway shape and dimensions were not taken into account; branches were considered to be correct as long as there was no significant leakage outside the airway walls. Since several annotations of the same images were evaluated, the evaluation process can be accelerated by automatically accepting branches that have high overlap with previously accepted branches. Finally, a reference segmentation was established by taking the union of all correct branches.

A diverse set of chest CT scans was contributed by eight different institutions. A total of 40 scans were selected, with 20 of these scans designated as training set, reserved for algorithm training and/or parameter tuning, and the remaining 20 as test set. The images were selected to include a large variety of acquisition conditions and pathologies.

The comparative study was organized as a challenge at the 2nd International Workshop on Pulmonary Image Analysis, which was held in conjunction with MICCAI 2009. Invitations to participate were sent out to several mailing lists and to authors of published papers on airway segmentation. Due to the time required for manual evaluation, participants were asked to submit results from a single method only. A total of 22 teams registered to download the data, and 15 teams [1–15] submitted their results, ten in the fully automated category and five in the semi-automated category. All results submitted by participating teams were used to establish the reference used for evaluation.

2 Data

A total of 75 chest CT scans were contributed by eight different sites. Scans were taken on several different CT scanner models, using a variety of scanning protocols and reconstruction parameters. The condition of the scanned subjects varied widely, ranging from healthy volunteers to patients showing severe pathology of the airways or lung parenchyma. Among the contributed CT scans, 40 were selected to be included into the dataset for the challenge, which were further divided into a training set and a test set. Care was taken to ensure that scans of all eight sites were represented in both the training and test sets, all files were anonymized properly, no scans of the same subject would be in both the training and test sets, and both sets included the same number of scans of similar quality, obtained at the same site and with similar characteristics. The 20 images in the training set were named CASE01 to CASE20, and the 20 images in the test set were named CASE21 to CASE40. Table 1 presents some characteristics of the 20 test cases.

Table 1. Acquisition parameters of the 20 test cases. Dosage is presented as x-ray tube current (kVp) and exposure (mAs) pair. The breathing status indicates full inspiration (Insp.) or full expiration (Exp.). Contrast indicates whether intravenous contrast was used during acquisition. The abbreviations for the scanner models are as follows: Siemens Sensation (SS), Siemens Volume Zoom (SVZ), Philips Mx8000 IDT (PMI), Philips Brilliance (PB), Toshiba Aquilion (TA) and GE LightSpeed (GEL). * indicates that the scan is from the same subject as the previous scan.

	Thickness (mm)	Scanner	Convolution Kernel	Dosage	Breath state	Contrast
CASE21	0.6	SS64	B50f	200/100	Exp.	No
CASE22*	0.6	SS64	B50f	200/100	Insp.	No
CASE23	0.75	SS64	B50f	200/100	Insp.	No
CASE24	1	TA	FC12	10/5	Insp.	No
CASE25*	1	TA	FC10	150/75	Insp.	No
CASE26	1	TA	FC12	10/5	Insp.	No
CASE27*	1	TA	FC10	150/75	Insp.	No
CASE28	1.25	SVZ	B30f	300/100	Insp.	Yes
CASE29*	1.25	SVZ	B50f	300/100	Insp.	Yes
CASE30	1	PMI16	D	120/40	Insp.	No
CASE31	1	PMI16	D	120/40	Insp.	No
CASE32	1	PMI16	D	120/40	Insp.	No
CASE33	1	SS16	B60f	321/200	Insp.	No
CASE34	1	SS16	B60f	321/200	Insp.	No
CASE35	0.625	GEL16	Std.	441/6209	Insp.	No
CASE36	1	PB16P	C	206/130	Insp.	No
CASE37	1	PB16P	B	64/30	Insp.	No
CASE38*	1	PB16P	C	51/20	Exp.	No
CASE39	1	SS16	B70f	436/205	Insp.	Yes
CASE40	1	SS16	B70s	162/105	Insp.	No

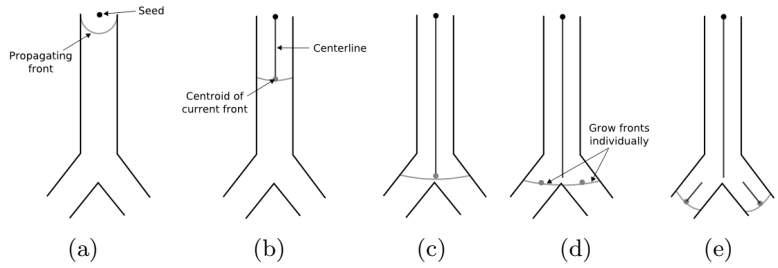

Fig. 1. Illustration of the process of dividing the airway tree into branches. (a) A seed point is set at the root of a tree and the front propagation process starts. (b) Centroid of the propagating front is stored as centerline at each time step. (c) The centerline is stored up to the point before a bifurcation. (d) Bifurcation is detected as the front splits. The individual fronts are used as seeds to perform front propagation in each of the branches. (e) Front propagation proceeds in each branch.

3 Airway branch evaluation

3.1 Subdividing an airway tree into branches

An important component of our evaluation is the process of subdividing an airway tree into its individual branch segments. This was done by detecting the bifurcations using wave front propagation, similar to [16]. The key idea is that a wave front propagating through a tree structure remains connected until it encounters a bifurcation, and any side branches can thus be detected as new disconnected components in the propagating front.

The front was propagated using a fast marching algorithm [17], with the speed function set to 1 within the segmented structure and 0 outside. We monitor the front through a set of "trial" points in the fast marching process. Connected component analysis was applied to the trial points when the time stamp from the fast marching algorithm increased by $1/\Delta D$, where ΔD is the distance between two voxels. Propagation stops when multiple disconnected components were detected in the front, whereupon the process was repeated on the individual split fronts to obtain the branches at the next level. The process ends when all marked regions of the tree have been evaluated. During the front propagation, the centerlines were obtained by storing the centroid of the front at every step. Figure 1 illustrates the algorithm.

3.2 Visual assessment

To enable visual inspection of extracted branches, each of the branches was presented to the trained observers using a fixed number of slices through the branch at different positions and orientations. Two different views were used, a reformatted and a reoriented view. The reformatted view was obtained by straightening the centerline of the branch segment, while the reoriented view

was obtained by rotating the branch segment such that its main axis coincides with the x-axis.

A total of eight slices were extracted from the reformatted view. The first four slices were taken perpendicular to the centerline, distributed evenly from the start to the end of the centerline. The other four slices were taken along the centerline, at cut planes that were angled at 0°, 45°, 90° and 135°. A schematic view of the cut planes for the different slices for the reformatted view is shown in Figure 2(b), with slice examples in Figure 2(d).

For the reoriented view, a total of nine slices were extracted, three from each axis. For the y-axis and z-axis, which are perpendicular to the axis of the branch segment, the cut planes were placed at 15%, 50% and 85% of the width of the branch measured in the respective axis. On the x-axis, the cut planes were placed at 5%, 50% and 95% of the length of the branch. Figure 2(b) shows the cut planes for the slices extracted from reoriented view, and examples of the slices are shown in Figure 2(e).

3.3 Evaluation of individual branches

Based on the slices from the two views described in Section 3.2, the trained observers were asked to assign one of the four following labels to each branch: "correct", "partly wrong", "wrong" or "unknown". A branch is "correct" if it does not have leakage outside the airway wall. "Partly wrong" is assigned to a branch if part of the branch lies well within the airway lumen, while part is outside the walls. A branch is "wrong" if it does not contain airway lumen at all. The "unknown" label is used when the observers are unable to determine whether a branch is an airway or not.

The evaluation of each branch was performed in two phases. At phase one, two observers are assigned to evaluate the branch. If both observers assign the same label, the evaluation is complete. Otherwise the evaluation proceeds to phase two, where three new observers are assigned. In this phase, the final label assigned to the branch is the label that constitutes the majority vote among the three new observers. In case of no majority, the branch is labeled as "unknown". The entire process was automated by web-based distribution of tasks to a pool of ten trained observers, who labeled the 15 segmentations of each of the 20 test cases. The observers were all medical students who were familiar with CT and chest anatomy. They were trained with a set of examples and subsequently processed two complete segmentations of different scans to ensure their ratings were reliable.

4 Establishing a reference

The reference segmentation for a CT scan was constructed by fusing branches based on the labels assigned as described in Section 3, which involves evaluated branches of segmented airway trees obtained from all participating teams.

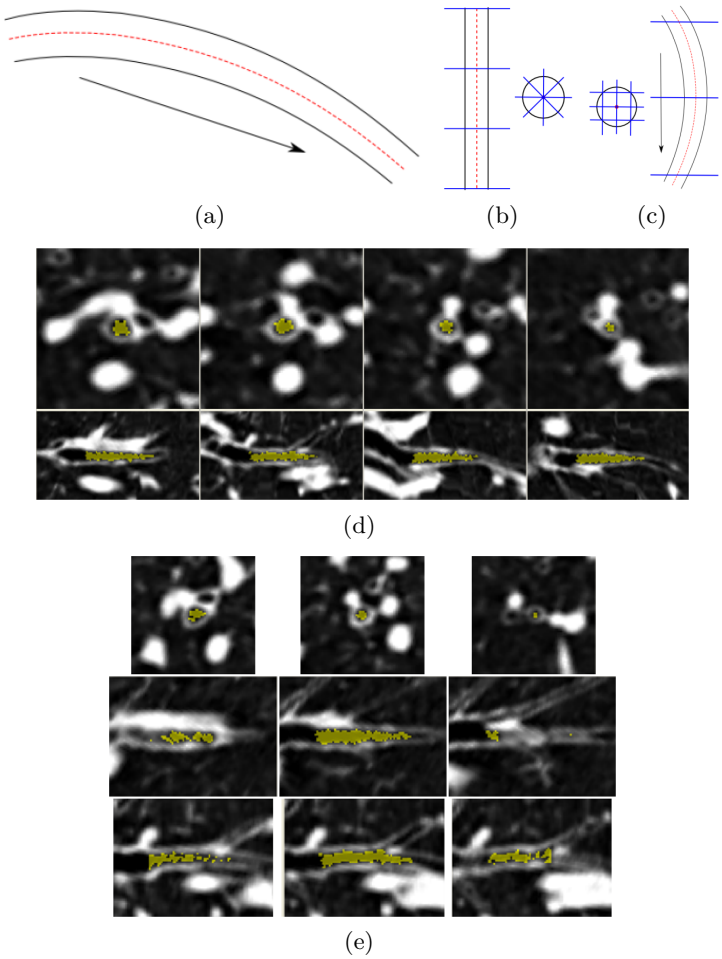

Fig. 2. Schematics showing the (a) original airway, (b) reformatted and (c) reoriented views. The arrow is the main orientation of the airway and the cut planes are shown in blue. Example of the slices extracted: (d) Reformatted view; top row are slices perpendicular to the branch segment and bottom row are slices taken in the direction of the branch segment. (e) Reoriented view; top row are axial slices, and middle and bottom row are cut planes parallel to the branch axis.

4.1 Automated branch acceptance

To speed up the evaluation process and reduce the number of branches that need to be evaluated by the observers, branches that were very similar to branches previously labeled "correct" were accepted automatically.

The following two criteria were used to determine whether to exempt a branch from manual evaluation or not:

1. Centerline overlap: Every point in the centerline is within a 26-neighborhood to a "correct" voxel.
2. Volume overlap: More than 80% of the voxels of the branch are labeled as "correct" in the reference.

Branches that fulfilled both criteria were labeled as "correct" and exempted from manual evaluation.

4.2 Updating the reference

The labels assigned by the observers as described in Section 3.3 and/or assigned automatically as above were subsequently stored in a reference image. The labels were stored as integer values with $L_c > L_w > L_p > L_u > 0$, where L_c, L_w, L_p and L_u represent the the values for "correct", "wrong", "partly wrong" and "unknown" respectively.

A reference image of a given CT scan started out as an empty image, with all voxels having value 0. Evaluated branches from a new segmentation of the same scan were added into the reference by applying the following update rule on all voxels $\boldsymbol{x}$

$$G_{t+1}(\boldsymbol{x}) = max\left(G_t(\boldsymbol{x}), L(\boldsymbol{x})\right),$$

where G_{t+1} and G_t are the reference after and before the update respectively, and L is the label assigned by the observers. The final reference of a CT scan was obtained once it was updated with all available evaluated segmentations.

4.3 Final reference

The final reference segmentation was defined as all voxels that were labeled as "correct" after updating the reference with all available evaluated segmentation results. Consequently, some of the voxels that were part of an airway lumen, but belonged to a branch segment containing errors and labeled "partly wrong", may be discarded. However, in our case, where a number of segmented airway trees from different algorithms are processed, the vast majority of airway voxels that were once labeled as "partly wrong" in an intermediate step are relabeled as they overlap with "correct" regions from another segmentation.

5 Evaluation

The algorithm described in Section 3.1 was used to obtain the centerlines of the branches in the reference segmentation. To enable comparison of the results obtained by different algorithms, we standardized the centerlines from the results to those of the reference segmentations. This was done by projecting the centerlines from a submitted result to the corresponding centerlines in the reference. The detected length of a given branch in the reference can then be obtained by measuring the length of the overlapping sections. To ensure that a branch is not trivially detected, a branch in the reference is said to be detected by a segmented airway tree only when the detected length is greater than $\Delta l = 1$ mm.

Seven performance measures were computed from the results of all participating teams:

1. Branch count: the number of branches that are detected correctly.
2. Branch detected: the fraction of branches that are detected, with respect to the total number of branches present in the reference.
3. Tree length: the sum of the length of the centerlines of all correctly detected branches.
4. Tree length detected: the fraction of tree length that is detected correctly relative to the reference.
5. Leakage count: the number of disconnected (26-connectivity) sources where leakage occurs. We define a leakage source as "correct" voxels that have at least a non-"correct" voxel within its 26-neighbors. A dilation of one voxel was applied to the detected sources prior to searching for the disconnected components in order to remove trivially disconnected sources.
6. Leakage volume: the volume of regions that are not marked as "correct" in the reference.
7. False positive rate: the fraction of the total segmented volume that is not marked as "correct" relative to the reference.

The trachea was excluded from measures $1-4$. For measures $5-7$, the trachea, left and right main bronchi were excluded.

6 Results

Table 2 presents the seven evaluation measures for the 15 participating teams, averaged over the 20 test cases. Figure 3(a) gives an overview of the average performance of the participating teams in terms of false positive rate over tree length detected, while Figure 3(b) shows the relation between the leakage volume and the number of leaks detected. Box plots of tree length detected and false positive rate for the different teams are given in Figure 4, while box plots for the number of branches detected and the leakage volume for each of the scans are given in Figure 5. In the box plots, the median is indicated by the red line, and the 25th and 75th percentile are indicated by the lower and upper edges of the box respectively. The lines below and above the box, or "whiskers", represent

the largest and smallest values that are within 1.5 times the interquartile range, while the red open circles show all outliers outside this range. Surface renderings from two cases are given in Figure 6 and 7, with correct and wrong regions indicated in green and red respectively.

Table 2. Average evaluation measures from each team average over the twenty cases in the test set. * indicates semi-automated category and best result for each measurement are indicated in bold.

	Branch count	Branch detected (%)	Tree length (cm)	Tree length detected (%)	Leakage count	Leakage volume (mm^3)	False positive rate (%)
Team [1]	91.1	43.5	64.6	36.4	2.5	152.3	1.27
Team [2]	157.8	62.8	122.4	55.9	12.0	563.5	1.96
Team [3]*	74.2	32.1	51.9	26.9	4.2	430.4	3.63
Team [4]	**186.8**	**76.5**	**158.7**	**73.3**	35.5	5138.2	15.56
Team [5]	150.4	59.8	118.4	54.0	1.9	18.2	0.11
Team [6]*	77.5	36.7	54.4	31.3	2.3	116.3	0.92
Team [7]	146.8	57.9	125.2	55.2	6.5	576.6	2.44
Team [8]*	71.5	30.9	52.0	26.9	0.9	126.8	1.75
Team [9]	139.0	56.0	100.6	47.1	13.5	368.9	1.58
Team [10]	79.3	32.4	57.8	28.1	**0.4**	**14.3**	**0.11**
Team [11]*	93.5	41.7	65.7	34.5	1.9	39.2	0.41
Team [12]	130.1	53.8	95.8	46.6	5.6	559.0	2.47
Team [13]	152.1	63.0	122.4	58.4	5.0	372.4	1.44
Team [14]	161.4	67.2	115.4	57.0	44.1	1873.4	7.27
Team [15]*	148.7	63.1	119.2	58.9	10.4	158.8	1.19

7 Discussions

As expected, there appears to be a trade off between sensitivity and specificity in the airway tree extraction, as can be observed from Figure 3(a) and Figure 4, where more complete trees are usually accompanied by a larger percentage of false positives. The most conservative algorithm is that of team [10], which obtains the smallest average leakage volume (14.3 mm^3) with one of the shortest trees (57.8 cm), while the algorithm of team [4] is the most explorative one, yielding the longest trees (158.7 cm) but at the expense of the largest leakage volume (5138.2 mm^3).

In general, the semi-automatic methods perform no better than the fully automatic methods. The manual interaction in most semi-automatic methods is limited to selecting initial seed points for the trachea [11, 8] or manually adapting parameters [6, 3]. An exception is the algorithm of [15], which allows for extensive editing of results.

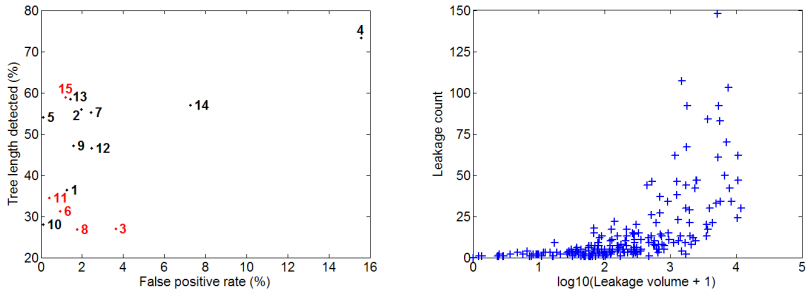

(a) (b)

Fig. 3. (a) Average false positive rate versus tree length detected of all participating teams, with teams in the semi-automated category in red. (b) Logarithm of leakage volume versus leakage count from all test cases results.

Figure 3(b) shows that the number of sources of leakage in an airway tree segmentation is often quite small. We found that over 66% of the submitted results have a leakage count of less than 5, with a maximum leakage volume of 1740.72 mm^3. This suggests that manually removing leakages from automatically extracted airway trees may be viable for most algorithms, provided that proper tools are available.

Interestingly, no algorithm came close to detecting the entire reference tree, as observed from Figure 4(a). The highest branch count and tree length detected for each case range from 64.6% to 94.3% and 62.6% to 90.4% respectively, with the average measures for each team no higher than 77%. This suggests that better results may be achieved by combining algorithms that use different approaches.

The box plots of the results per test case in Figure 5 reveal that in general, ultra low dose scans (cases 24, 26, 37, and 38) are more difficult to segment than low dose or clinical dose scans. From these scans, significantly fewer branches were extracted ($p < 0.01$ from Student's t-tests) with no significant difference in leakage volume ($p = 0.10$). For the two pairs of low dose and ultra low dose scans (case 24, 25 and 26, 27), branch count were significantly higher ($p < 0.01$ from paired Student's t-tests) for the low dose scans (93 branches) than for the ultra low dose (73 branches) scans, while there was no significant difference in leakage volume ($p = 0.54$).

From the available paired inspiration and expiration scans (case 21, 22 and 37, 38), segmentations of the inspiration scans include more correct branches but also more leakage than their expiration counterparts, where inspiration scans exhibits an average branch count of 145 branches and leakage volume of 942 mm^3 as compared to 76 branches and 115 mm^3 from expiration scans. A paired Student's t-tests shows that these difference are indeed significant, with $p < 0.01$ for both branch count and $p = 0.02$ for leakage volume.

One image pair, cases 28 and 29, is the same scan reconstructed using a soft and a hard kernel. For these scans, significantly more branches ($p < 0.01$)

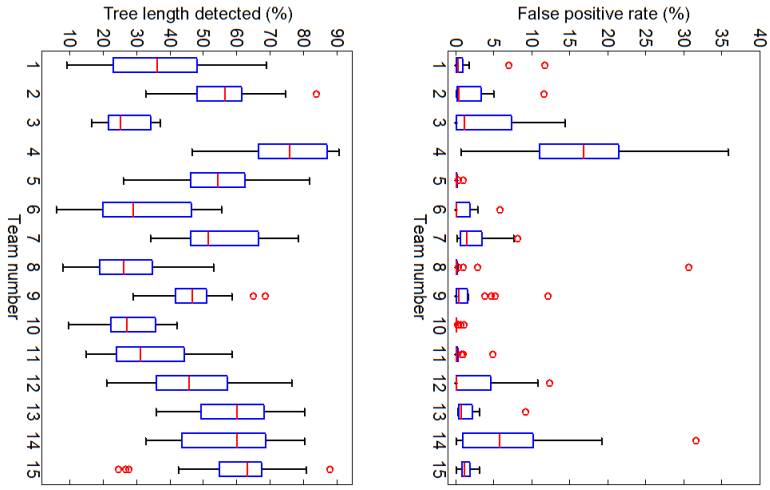

(a) (b)

Fig. 4. Box plots of (a) tree length detected and (b) false positive rate of the teams.

were extracted from the scan constructed using the hard kernel, average of 106 branches compared to 80 branches. Although average leakage volume for hard kernel scan was higher, 418 mm^3 compared to 236 mm^3, the difference was not significant ($p = 0.30$).

8 Conclusion

A framework for evaluating airway extraction algorithms in a standardized manner and establishing a reference segmentation is presented. Results obtained by 15 different airway tree extraction algorithms on a diverse set of 20 chest CT scans were manually evaluated and a reference was constructed from all correctly segmented branches. A total of seven performance measures were computed for each of the algorithms using the constructed reference. Results showed that no algorithm is capable of extracting more than 77% of the reference, in terms of both branch count and tree length, on average, indicating that better results may be achieved by combining results from different algorithms.

Acknowledgments. We would like to thank the following people for contributing data to this study:

– Haseem Ashraf and Asger Dirksen (Gentofte University Hospital, Denmark)
– Jesper Pedersen (Rigshospitalet - Copenhagen University Hospital, Denmark)

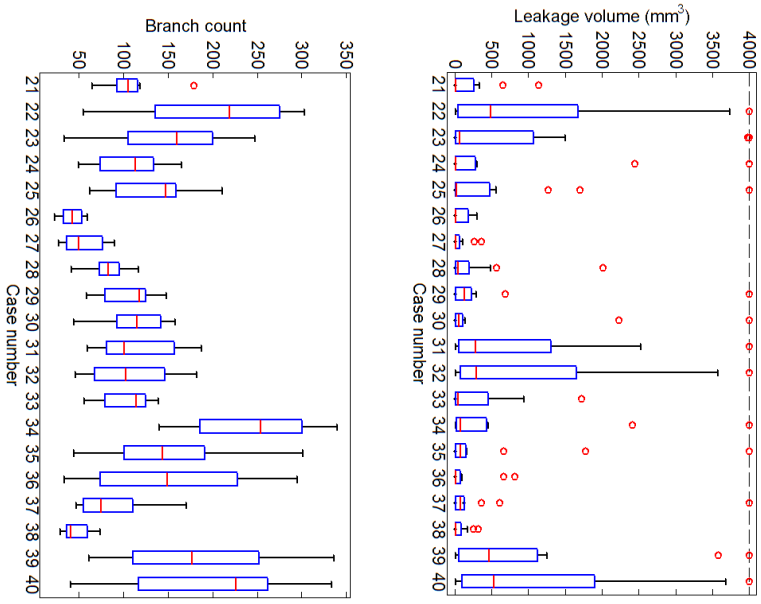

(a) (b)

Fig. 5. Box plots of (a) branch count and (b) leakage volume, with the maximum leakage volume clipped at 4000 mm^3, of the 20 test cases.

– Patrik Rogalla (Charité, Humboldt University Berlin, Germany)
– Jan-Martin Kuhnigk (Fraunhofer MEVIS, Germany)
– Rafael Wiemker, Cristian Lorenz (Philips Research Lab Hamburg, Germany)
– Berthold Wein (University Hospital of Aachen, Germany)
– Ken Mori (Graduate School of Information Science Nagoya University, Japan)
– Ieneke Hartmann (Erasmus MC - University Medical Center Rotterdam, The Netherlands)
– Eric Hoffman (Department of Radiology, University of Iowa, USA)
– Atilla Kiraly, Carol Novak, Benjamin Odry (Siemens Corporate Research, USA)
– David Naidich (NYU Medical Center, USA)
– Mathias Prokop (University Medical Center Utrecht, the Netherlands)

We also thank all participants of EXACT'09 and the ten trained observers for making this evaluation possible.

This work was funded in part by the Danish Council for Strategic Research (NABIIT), the Netherlands Organization for Scientific Research (NWO), and by grants HL080285 and HL079406 from the U.S. National Institutes of Health.

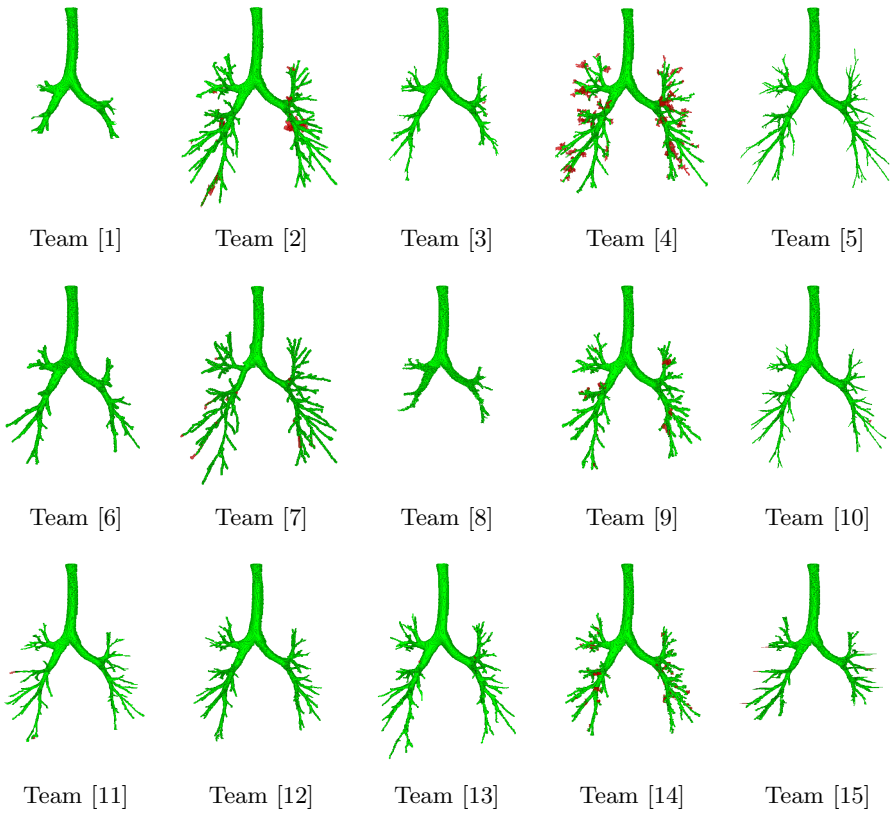

Fig. 6. Surface renderings of results for case 23, with correct and wrong regions shown in green and red respectively.

References

1. Irving, B., Taylor, P., Todd-Pokropek, A.: 3D segmentation of the airway tree using a morphology based method. In: Proc. of Second International Workshop on Pulmonary Image Analysis. (2009)
2. Fetita, C., Ortner, M., Brillet, P.Y., Prêteux, F., Grenier, P.: A morphological-aggregative approach for 3D segmentation of pulmonary airways from generic MSCT acquisitions. In: Proc. of Second International Workshop on Pulmonary Image Analysis. (2009)
3. Pinho, R., Luyckx, S., Sijbers, J.: Robust region growing based intrathoracic airway tree segmentation. In: Proc. of Second International Workshop on Pulmonary Image Analysis. (2009)
4. Feuerstein, M., Kitasaka, T., Mori, K.: Adaptive branch tracing and image sharpening for airway tree extraction in 3-D chest CT. In: Proc. of Second International Workshop on Pulmonary Image Analysis. (2009)
5. Lo, P., Sporring, J., de Bruijne, M.: Multiscale vessel-guided airway tree segmentation. In: Proc. of Second International Workshop on Pulmonary Image Analysis. (2009)

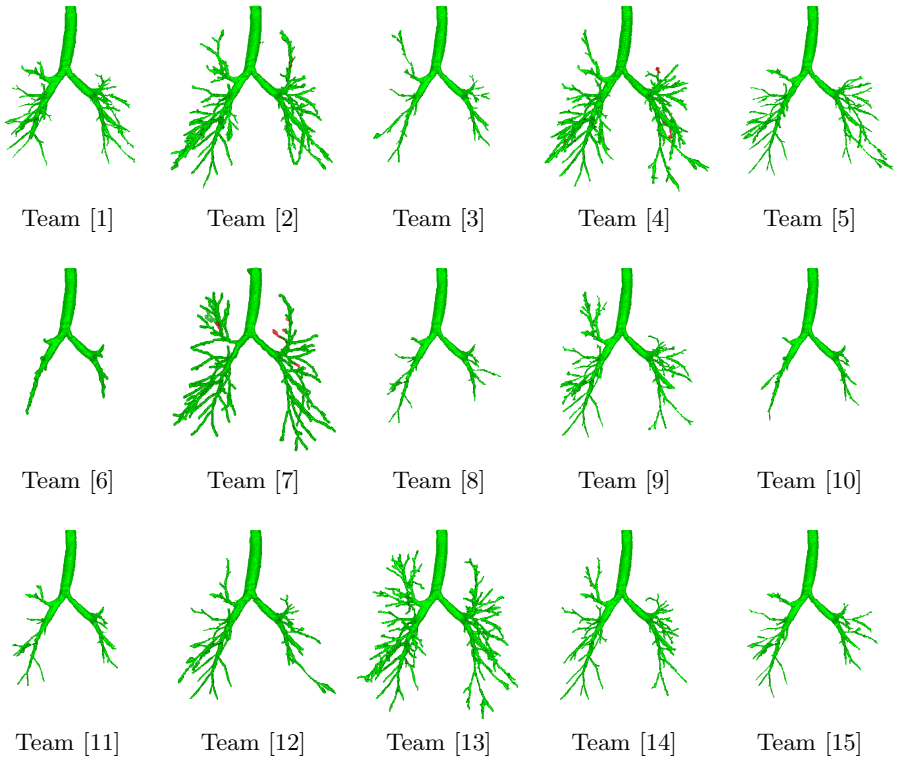

Fig. 7. Surface renderings of results for case 36, with correct and wrong regions shown in green and red respectively.

6. Fabijanska, A.: Results of applying two-pass region growing algorithm for airway tree segmentation to MDCT chest scans from EXACT database. In: Proc. of Second International Workshop on Pulmonary Image Analysis. (2009)
7. Bauer, C., Pock, T., Bischof, H., Beichel, R.: Airway tree reconstruction based on tube detection. In: Proc. of Second International Workshop on Pulmonary Image Analysis. (2009)
8. Mendoza, C.S., Acha, B., Serrano, C.: Maximal contrast adaptive region growing for CT airway tree segmentation. In: Proc. of Second International Workshop on Pulmonary Image Analysis. (2009)
9. Wiemker, R., Buelow, T., Lorenz, C.: A simple centricity-based region growing algorithm for the extraction of airways. In: Proc. of Second International Workshop on Pulmonary Image Analysis. (2009)
10. Lee, J., Reeves, A.P.: Segmentation of the airway tree from chest CT using local volume of interest. In: Proc. of Second International Workshop on Pulmonary Image Analysis. (2009)
11. Born, S., Iwamaru, D., Pfeifle, M., Bartz, D.: Three-step segmentation of the lower airways with advanced leakage-control. In: Proc. of Second International Workshop on Pulmonary Image Analysis. (2009)

12. Weinheimer, O., Achenbach, T., Düber, C.: Fully automated extraction of airways from CT scans based on self-adapting region growing. In: Proc. of Second International Workshop on Pulmonary Image Analysis. (2009)
13. Bauer, C., Bischof, H., Beichel, R.: Segmentation of airways based on gradient vector flow. In: Proc. of Second International Workshop on Pulmonary Image Analysis. (2009)
14. van Rikxoort, E.M., Baggerman, W., van Ginneken, B.: Automatic segmentation of the airway tree from thoracic CT scans using a multi-threshold approach. In: Proc. of Second International Workshop on Pulmonary Image Analysis. (2009)
15. Tschirren, J., Yavarna, T., Reinhardt, J.: Airway segmentation framework for clinical environments. In: Proc. of Second International Workshop on Pulmonary Image Analysis. (2009)
16. Schlathölter, T., Lorenz, C., Carlsen, I.C., Renisch, S., Deschamps, T.: Simultaneous segmentation and tree reconstruction of the airways for virtual bronchoscopy. Volume 4684., SPIE (2002) 103–113
17. Malladi, R., Sethian, J.: Level set and fast marching methods in image processing and computer vision. In: Proc. International Conference on Image Processing. Volume 1. (1996) 489–492 vol.1